Theory on Phase Behavior of Triblocklike Supramolecules Formed from Reversibly Associating End-functionalized Polymer Blends

June Huh and Won Ho Jo*

Hyperstructured Organic Materials Research Center, and School of Materials Science and Engineering, Seoul National University, Seoul 151-742, Korea

Received June 29, 2003; Revised Manuscript Received January 12, 2004

ABSTRACT: The phase behavior of blends of mono-end-functionalized polymers (denoted by A) and a di-end-functionalized polymer (denoted by B), capable of forming triblocklike supramolecules, is theoretically predicted by using a weak-segregation theory based on the Landau formalism. In this model system, polymers can form diblocklike or triblocklike clusters via associations between end-functionalized groups of A- and B-homopolymers. The free energies of various ordered structures including complex phases such as gyroid and double diamond are calculated within the second-harmonic approximation and the possibility of phase coexistences is examined. It is found that the blends of these functionalized polymers exhibit various phase behaviors including closed loop phase boundary of biphasic coexistence. We also discuss about the stability of cylindrical phase arranged with square symmetry competed with hexagonally arranged cylindrical phase by using a multiple harmonics approach up to the third harmonics.

I. Introduction

Block copolymers exhibit various ordered structures with a periodicity of 10−100 nm owing to the self-organization driven by the incompatibility between chemically linked blocks.[1−3] This behavior of block copolymers can be used in molecular engineering to render the structure of the copolymers controllable in nanoscales. Very recently, as an alternative to obtaining nanosized periodic structures, the formation of block copolymer-like molecular clusters due to physical bonding such as hydrogen bonding or ionic interactions has attracted much attention. In this case, the self-organizing units are not chemically bonded, and thus the self-organized clusters can be regarded as physically bonded supramolecules. A number of recent experimental reports show that this kind of physically bonded clusters offers a particularly facile way to construct self-organized materials with one or more characteristic length scales.[4−8] One of the examples is provided by Ruokolainen et al.[9] on a mixture of poly(4-vinylpyridine) (P4VP) and end-functionalized oligomers, which can form comb copolymer-like clusters due to hydrogen bonding between end functional groups of oligomers and the nitrogen of the pyridine groups of P4VP. As a similar approach, a blend of functionalized polystyrene (PS) having dimethylamino groups at one end and polyisoprene (PI) one-end-capped by sulfonic acid has been studied by Pipas et al.[10] They have shown that miktoarm block copolymer-like clusters are formed by ionic interactions via proton transfer from sulfonic acid groups of PI to the tertiary amine groups of PS and exhibit various ordered structures depending on the mixing ratio of PS to PI.

A theory for such associating polymer mixtures has been first developed by Tanaka and co-workers[11−13] and the essential physical principle underlying phase behavior is established by a mean-field theory. Although the theory predicts some general features of associating mixture such as spinodal instability for micro- and macrophase separation, the free energy of the microstructure due to the presence of block copolymer-like clusters is not considered and thus the relative stability of detailed ordered structures cannot be examined. To complete this limited prediction, ten Brinke and co-workers[14,15] have advanced the theory by taking into account the free energy of microstructure based on the Landau free energy expansion and examined the stability of ordered structures within a first harmonic approximation. In their theory, the free energy for the mixture containing clusters is expressed in terms of the distribution of clusters and the parameters describing microstructures, i.e., period, amplitude of concentration fluctuation, and symmetry of microstructure. Since the cluster distribution is dependent on temperature, the free energy has to be minimized *simultaneously* with respect to the cluster distribution and with respect to the parameters describing its microstructure. This minimization procedure seems very complicated when compared to that for mixtures of covalently bonded block copolymers where the composition of molecular species is fixed. The most notable theoretical progress is achieved in ref 15. They have shown that the simultaneous minimization procedure for cluster systems can be replaced by a stepwise minimization. By using this simplification of the minimization procedure, they are able to construct the phase diagram for A/B binary blend forming the diblocklike cluster as a simple example of an associating mixture. However, since the free energies of phase structures in their approach are expressed within the first harmonic approximation, the predictions about ordered structures are limited to classical phases of lamellar, hexagonal, and body-centered cubic structures, and consequently the possibility of other structures such as bicontinuous structures, e.g. double gyroid, was excluded. Therefore, for a more mature approach, it is now necessary to develop the theory by taking into account various complex ordered structures, which provides us with the motivation for the present work.

Our primary objectives of this study are first to develop a theory for phase behavior of blends of A-polymers functionalized at one end and B-polymers functionalized at both ends and then to predict their phase struc-

* To whom correspondence should be addressed. Telephone: 82-2−880-7192. Fax: 82-2-885-1748. E-mail: whjpoly@plaza.snu.ac.kr.

10.1021/ma034895m CCC: $27.50
Published on Web 03/19/2004

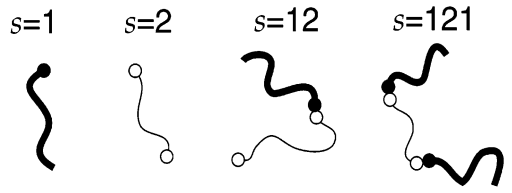

Figure 1. Schematic representation of four different molecular states ($s = 1$, $s = 2$, $s = 12$, $s = 121$).

tures using a weak segregation theory. In the model system under study the association can occur only between an end-functional group in the A-chain and an end-functional group in the B-chain and not between functionalized groups belonging to the same molecular species. The resulting molecular clusters via associations therefore resemble diblock or triblock copolymers. To predict phase structures of the mixtures, the free energies of ordered structures are obtained within a second harmonic approximation. The harmonic corrections by the second harmonic approximation allow us to investigate various ordered structures including nonclassical structures.

This paper is organized as follows. In the next section, we describe the weak segregation theory based upon the Landau−Ginzburg formalism for associating polymer mixtures capable of forming triblocklike clusters. In section III, the calculated phase diagrams are presented and their phase structures are discussed. In the final section, we summarize our main findings and provide a short discussion of some features of the predicted phase diagrams.

II. Theory

We consider a molten binary blend of functionalized A- and B-homopolymer consisting of N and αN monomers, respectively. Each of the A-polymers has a functionalized group at one end and each of the B-polymers has functionalized groups at both ends. It is further assumed that a functionalized monomer of A-chain can associate only with a functionalized monomer of B-chain and thus the self-association between two A-chains or between two B-chains is not allowed. Therefore, the following molecular states are possible as a result of the association between chain molecules: free A-chains, free B-chains, diblocklike clusters, and triblocklike clusters. Figure 1 presents the schematic representation for the four different molecular states possible in this system. In the remainder of this paper, each of the molecular states is denoted by the numerals 1 (free A-chain), 2 (free B-chain), 12 (diblocklike cluster), and 121 (triblocklike cluster), while the alphabetic notation of A or B denotes the monomer type.

The free energy change of the model system under study, ΔF, can be expressed by the sum of two terms:

$$\Delta F = \Delta F_{\mathrm{h}} + \Delta F_{\mathrm{micro}} \tag{1}$$

where ΔF_{h} is the free energy difference between homogeneous state of the mixture and a reference state of pure components, and $\Delta F_{\mathrm{micro}}$ is the free energy difference between the homogeneous state and a microscopically phase-separated state. Assuming that the system is incompressible, the free energy change of the homogeneous state for the mixture containing clusters is given as

$$\frac{N\Delta F_{\mathrm{h}}}{Vk_{\mathrm{B}}T} = \left(\frac{\phi_{12}}{1+\alpha} + \frac{2\phi_{121}}{2+\alpha}\right)\left(1 + \frac{f_{\mathrm{b}}}{k_{\mathrm{B}}T} - \ln(z-1)\right) + \frac{\phi_{12}}{1+\alpha}\ln\frac{N\alpha}{1+\alpha} + \frac{\phi_{121}}{2+\alpha}\ln\frac{N^2\alpha}{2+\alpha} + \phi_1 \ln \phi_1 + \frac{\phi_2}{\alpha}\ln\phi_2 + \frac{\phi_{12}}{1+\alpha}\ln\phi_{12} + \frac{\phi_{121}}{2+\alpha}\ln\phi_{121} + N\chi\phi(1-\phi) \tag{2}$$

where V is the system volume, f_{b} is the free energy change associated with the formation of a single *physical bonding* between a pair of associating functionalized monomers, ϕ_i is the volume fraction of species type i ($i = 1, 2, 12, 121$), ϕ is the volume fractions of A-chains, z is the coordination number, and χ is the Flory interaction parameter between A- and B-monomers. The first term in eq 2 accounts for the free energy contribution due to the formation of diblocklike and triblocklike clusters and the remaining terms represent the contribution due to mixing of free and associated species. In deriving eq 2, it is important to recognize that the reference state is *not* the state of a priori made free and associated species (1, 2, 12, and 121) but the state of pure homopolymers (A and B). Therefore, the free energy change of the homogeneous phase, ΔF_{h}, must contains an entropic contribution due to the various ways of combining the A- and B-chains to form the clusters since the associations between polymers are not permanent. Therefore, the system can be regarded as an *annealed* system, whereas a covalently bonded block copolymer melt is a *quenched* system since the bonds are permanent.

The second contribution, $\Delta F_{\mathrm{micro}}$, can be expressed in terms of the order parameter $\Psi(\mathbf{r})$ that represents the local density deviation of A-monomers. In the weak segregation regime where the order parameter is small, $\Delta F_{\mathrm{micro}}$ is approximated by the Landau expansion in powers of the order parameter up to the fourth order:[16]

$$\frac{\Delta F_{\mathrm{micro}}}{k_{\mathrm{B}}T} = \sum_{n=2}^{4}\frac{1}{n!V^n}\int \mathrm{d}\mathbf{q}_1 \dots \int \mathrm{d}\mathbf{q}_n \Gamma_n(\mathbf{q}_1,\dots,\mathbf{q}_n) \times \Psi(\mathbf{q}_1)\dots\Psi(\mathbf{q}_n) \tag{3}$$

where $\Psi(\mathbf{q})$ is the Fourier transform of the order parameter representing the A-monomer density profile having a period of $2\pi/|\mathbf{q}|$. The Landau free energy expressed in eq 3 depends on the molecular architectures via the vertex function, Γ_n. The formulas for the vertex functions can be obtained from the random phase approximation (RPA) which gives

$$\Gamma_2(\mathbf{q}_1,\mathbf{q}_2) = V\delta(\mathbf{q}_1+\mathbf{q}_2) \times \left[\frac{\bar{g}_{\mathrm{AA}}(\mathbf{q}_1) + \bar{g}_{\mathrm{BB}}(\mathbf{q}_1) + 2\bar{g}_{\mathrm{AB}}(\mathbf{q}_1)}{\bar{g}_{\mathrm{AA}}(\mathbf{q}_1)\bar{g}_{\mathrm{BB}}(\mathbf{q}_1) - \bar{g}_{\mathrm{AB}}{}^2(\mathbf{q}_1)} - 2\chi\right] \tag{4}$$

$$\Gamma_3(\mathbf{q}_1,\mathbf{q}_2,\mathbf{q}_3) = -V\delta(\mathbf{q}_1+\mathbf{q}_2+\mathbf{q}_3)\bar{g}_{ijk}(\mathbf{q}_1,\mathbf{q}_2,\mathbf{q}_3) \times [\bar{g}_{i\mathrm{A}}{}^{-1}(\mathbf{q}_1) - \bar{g}_{i\mathrm{B}}{}^{-1}(\mathbf{q}_1)][\bar{g}_{j\mathrm{A}}{}^{-1}(\mathbf{q}_2) - \bar{g}_{j\mathrm{B}}{}^{-1}(\mathbf{q}_2)] \times [\bar{g}_{k\mathrm{A}}{}^{-1}(\mathbf{q}_3) - \bar{g}_{k\mathrm{B}}{}^{-1}(\mathbf{q}_3)] \tag{5}$$

$$\Gamma_4(\mathbf{q}_1,\mathbf{q}_2,\mathbf{q}_3,\mathbf{q}_4) = \Gamma_4^{\mathrm{reg}} + \Gamma_4^{\mathrm{nl}}$$

$$= V\delta(\mathbf{q}_1+\mathbf{q}_2+\mathbf{q}_3+\mathbf{q}_4)[\gamma_{ijkl}^{\mathrm{reg}}(\mathbf{q}_1,\mathbf{q}_2,\mathbf{q}_3,\mathbf{q}_4) + \gamma_{ijkl}^{\mathrm{nl}}(\mathbf{q}_1,\mathbf{q}_2,\mathbf{q}_3,\mathbf{q}_4)][\bar{g}_{i\mathrm{A}}{}^{-1}(\mathbf{q}_1) - \bar{g}_{i\mathrm{B}}{}^{-1}(\mathbf{q}_1)][\bar{g}_{j\mathrm{A}}{}^{-1}(\mathbf{q}_2) - \bar{g}_{j\mathrm{B}}{}^{-1}(\mathbf{q}_2)][\bar{g}_{k\mathrm{A}}{}^{-1}(\mathbf{q}_3) - \bar{g}_{k\mathrm{B}}{}^{-1}(\mathbf{q}_3)][\bar{g}_{l\mathrm{A}}{}^{-1}(\mathbf{q}_4) - \bar{g}_{l\mathrm{B}}{}^{-1}(\mathbf{q}_4)] \tag{6}$$

where

$$\gamma^{\mathrm{reg}}_{ijkl}(\mathbf{q}_1,\mathbf{q}_2,\mathbf{q}_3,\mathbf{q}_4) = -\bar{g}_{ijkl}(\mathbf{q}_1,\mathbf{q}_2,\mathbf{q}_3,\mathbf{q}_4) + \bar{g}_{iju}(\mathbf{q}_1,\mathbf{q}_2,-\mathbf{q}_1-\mathbf{q}_2)\bar{g}_{uv}^{-1}(\mathbf{q}_1+\mathbf{q}_2)\bar{g}_{klv}(\mathbf{q}_3,\mathbf{q}_4,-\mathbf{q}_3-\mathbf{q}_4) + \bar{g}_{iku}(\mathbf{q}_1,\mathbf{q}_3,-\mathbf{q}_1-\mathbf{q}_3)\bar{g}_{uv}^{-1}(\mathbf{q}_1+\mathbf{q}_3)\bar{g}_{jlv}(\mathbf{q}_2,\mathbf{q}_4,-\mathbf{q}_2-\mathbf{q}_4) + \bar{g}_{ilu}(\mathbf{q}_1,\mathbf{q}_4,-\mathbf{q}_1-\mathbf{q}_4)\bar{g}_{uv}^{-1}(\mathbf{q}_1+\mathbf{q}_4)\bar{g}_{jkv}(\mathbf{q}_2,\mathbf{q}_3,-\mathbf{q}_2-\mathbf{q}_3) \quad (7)$$

$$\gamma^{\mathrm{nl}}_{ijkl}(\mathbf{q}_1,\mathbf{q}_2,\mathbf{q}_3,\mathbf{q}_4) = \delta(\mathbf{q}_1+\mathbf{q}_2)\delta(\mathbf{q}_3+\mathbf{q}_4) \sim [\overline{g_{ij}(\mathbf{q}_1)g_{kl}(\mathbf{q}_3)} - \bar{g}_{iju}(\mathbf{q}_1,\mathbf{q}_2,-\mathbf{q}_1-\mathbf{q}_2)\bar{g}_{uv}^{-1}(\mathbf{q}_1+\mathbf{q}_2)\bar{g}_{klv}(\mathbf{q}_3,\mathbf{q}_4,-\mathbf{q}_3-\mathbf{q}_4)] + \delta(\mathbf{q}_1+\mathbf{q}_3)\delta(\mathbf{q}_2+\mathbf{q}_4) \times [\overline{g_{ik}(\mathbf{q}_1)g_{jl}(\mathbf{q}_2)} - \bar{g}_{iku}(\mathbf{q}_1,\mathbf{q}_3,-\mathbf{q}_1-\mathbf{q}_3)\bar{g}_{uv}^{-1}(\mathbf{q}_1+\mathbf{q}_3)\bar{g}_{jlv}(\mathbf{q}_2,\mathbf{q}_4,-\mathbf{q}_2-\mathbf{q}_4)] + \delta(\mathbf{q}_1+\mathbf{q}_4)\delta(\mathbf{q}_2+\mathbf{q}_3) \times [\overline{g_{ik}(\mathbf{q}_1)g_{jl}(\mathbf{q}_2)} - \bar{g}_{ilu}(\mathbf{q}_1,\mathbf{q}_4,-\mathbf{q}_1-\mathbf{q}_4)\bar{g}_{uv}^{-1}(\mathbf{q}_1+\mathbf{q}_4)\bar{g}_{jkv}(\mathbf{q}_2,\mathbf{q}_3,-\mathbf{q}_2-\mathbf{q}_3)] \quad (8)$$

In eqs 5−8, the Einstein convention for summation over repeated indices has been used. The averages of the correlation functions, $\bar{g}$ and $\overline{g_{ij}g_{kl}}$, are given from the monomer density correlation functions of a single Gaussian chain of species s, g^s:

$$\bar{g}_{ij}... = \sum_s \frac{\phi_s}{N_s} g^s_{ij}... \quad (9)$$

$$\overline{g_{ij}g_{kl}} = \sum_s \frac{\phi_s}{N_s} g^s_{ij}g^s_{kl} \quad (10)$$

The formulas for $\bar{g}$ are given in Appendix A. In eqs 5−8, the $\bar{g}_{ij}^{-1}$ represents the ij component of the inverse of the matrix, $\bar{g}_{ij}$. It should be mentioned that when the theory is applied to the blends containing clusters, a cluster formed by associations between A- and B-homopolymers is treated as a single molecular species so that the vertex functions in eqs 4−6 have the contributions from associated *pseudomolecules*, which behave as diblock or triblock copolymers. In relation to this, a special attention must be given to the fourth order vertex function, Γ_4, which has a contribution of Γ_4^{nl}.[17−19] This so-called "nonlocal" contribution accounts for an entropic penalty due to the molecular dissimilarity between different species participating in formation of an ordered state and vanishes for the melt consisting of only one kind of molecular species. For the annealed system, like the associating blends, this nonlocal contribution can be omitted in connection with minimization of free energy, which will be discussed later in this section.

The order parameter $\Psi(\mathbf{q})$ in eq 3 can be expressed in terms of the symmetry of ordered structures and is expanded as

$$\Psi(\mathbf{q}) = \sum_{a=1}^{\infty} \frac{V}{\sqrt{n_a}} A_a \sum_{k=1}^{n_a} \exp(i\varphi_{k,a})\delta(\mathbf{Q}_{k,a} - \mathrm{q}) \quad (11)$$

where A_a, $\varphi_{k,a}$, and n_a are the amplitude, the phase, and the half-number of wave vectors in the ath harmonic shell for an ordered structure having $\{\mathbf{Q}_{k,a}\}$ wave vectors in the reciprocal lattice, respectively. When the harmonic contributions are considered up to mth shell, each order term in the free energy of microstructure can then be rewritten as

$$\frac{\Delta F^{(2)}_{\mathrm{micro}}}{Vk_{\mathrm{B}}T} = \sum_{a=1}^{m} \Gamma_2(Q_a){A_a}^2 \quad (12)$$

$$\frac{\Delta F^{(3)}_{\mathrm{micro}}}{Vk_{\mathrm{B}}T} = \frac{1}{3!}\sum_{a=1}^{m}\sum_{b=1}^{m}\sum_{c=1}^{m}\sum_{i}^{2n_a}\sum_{j}^{2n_b}\sum_{k}^{2n_c}\Gamma_3(\mathbf{Q}_{i,a},\mathbf{Q}_{j,b},\mathbf{Q}_{k,c}) \times \left(\frac{A_aA_bA_c}{\sqrt{n_an_bn_c}}\right)\mathrm{e}^{i(\varphi_{i,a}+\varphi_{j,b}+\varphi_{k,c})} \quad (13)$$

$$\frac{\Delta F^{(4)}_{\mathrm{micro}}}{Vk_{\mathrm{B}}T} = \frac{1}{4!}\sum_{a=1}^{m}\sum_{b=1}^{m}\sum_{c=1}^{m}\sum_{d=1}^{m}\sum_{i=1}^{2n_a}\sum_{j=1}^{2n_b}\sum_{k=1}^{2n_c}\sum_{l=1}^{2n_d}\Gamma_4 \times (\mathbf{Q}_{i,a},\mathbf{Q}_{j,b},\mathbf{Q}_{k,c},\mathbf{Q}_{l,d})\left(\frac{A_aA_bA_cA_d}{\sqrt{n_an_bn_cn_d}}\right)\mathrm{e}^{i(\varphi_{i,a}+\varphi_{j,b}+\varphi_{k,c}+\varphi_{l,d})} \quad (14)$$

where $\Delta F^{(n)}_{\mathrm{micro}}$ is the nth order contribution of the free energy expansion of eq 3 and $Q_a = |\mathbf{Q}_{i,a}|$. In applying the formula of eq 11 to the Landau free energy, the cutoff in the harmonic shells is of crucial importance. In the original theory for block copolymer developed by Leibler,[16] the expansion in eq 11 is restricted to the first shell of reciprocal lattice, i.e., the first harmonic approximation, and as a consequence, the mathematical procedure for minimization of the free energy of microstructure is greatly simplified. From the physical point of view, the first harmonic approach is justified in the limit that the composition profile $\Psi(\mathbf{r})$ is perfectly sinusoidal. In reality, however, the composition profile consists of more than one length scale and its scattering pattern shows higher-order reflections. Also, the most critical drawback of the first harmonic approach is that it predicts only three classical phases of flat lamellae, hexagonally packed cylinders, and spheres arranged on body-centered cubic lattices, while real systems are known to form much more various structures such as bicontinuous cubic structures. To overcome this limitation, the so-called "harmonic corrections" is used by including the higher harmonics.[20−23] In this work, the second harmonic corrections are taken into account by considering the harmonics with $Q_2 \le 2^{1/2}Q_1$. Within this approximation, only one harmonic should be used for the lamellar structure ($Q_2/Q_1 = 2$) and the hexagonally packed cylindrical structure ($Q_2/Q_1 = 3^{1/2}$) while the other structures are represented by two-harmonic density profile. Inserting the order parameter expressed by two-harmonic representation into eq 3, the free energy of microstructure has the form of

$$\frac{\Delta F_{\mathrm{micro}}}{Vk_{\mathrm{B}}T} = \Gamma_2(Q_1){A_1}^2 + \Gamma_2(Q_2){A_2}^2 + \nu_{111}{A_1}^3 + 3\nu_{112}{A_1}^2A_2 + 3\nu_{122}A_1{A_2}^2 + \nu_{222}{A_2}^3 + \lambda_{1111}{A_1}^4 + 4\lambda_{1112}{A_1}^3A_2 + 6\lambda_{1122}{A_1}^2{A_2}^2 + 4\lambda_{2221}A_1{A_2}^3 + \lambda_{2222}{A_2}^4 \quad (15)$$

with the following structure-dependent parameters:

$$\nu_{abc} = \frac{1}{3!\sqrt{n_a n_b n_c}} \sum_{i=1}^{2n_a}\sum_{j=1}^{2n_b}\sum_{k=1}^{2n_c} \Gamma_3(\mathbf{Q}_{i,a},\mathbf{Q}_{j,b},\mathbf{Q}_{k,c}) e^{i(\varphi_{i,a}+\varphi_{j,b}+\varphi_{k,c})} \tag{16a}$$

$$\lambda_{abcd} = \frac{1}{4!\sqrt{n_a n_b n_c n_d}} \sum_{i=1}^{2n_a}\sum_{j=1}^{2n_b}\sum_{k=1}^{2n_c}\sum_{l=1}^{2n_d} \Gamma_4 \times (\mathbf{Q}_{i,a},\mathbf{Q}_{j,b},\mathbf{Q}_{k,c},\mathbf{Q}_{l,d}) e^{i(\varphi_{i,a}+\varphi_{j,b}+\varphi_{k,c}+\varphi_{l,d})} \tag{16b}$$

Using the harmonic corrections discussed above, the following structures are considered in this work: lamellae (L); hexagonally packed cylinders (H); cylinders arranged on square lattice (SQ); spheres arranged on body-centered cubic lattice (B); spheres arranged on face-centered cubic lattice (F); spheres arranged on simple cubic lattice (SC); hexagonally perforated layers (HPL); bicontinuous double gyroid (G) with $Ia\bar{3}d$ space-group symmetry; bicontinuous double diamond (OBDD) with $Pn\bar{3}m$ symmetry. The ν_{abc} and λ_{abcd} for ordered structures considered in this study are listed in Appendix B.

To construct the phase diagram for the mixture, the total free energy expressed in eq 1 should be minimized simultaneously with respect to the cluster distribution $\{\phi_s\}$ and with respect to the parameters of ordered structure, i.e., period, amplitudes, phases, and type of ordered structure:

$$\Delta F^{**} = \min_{x,y}[\Delta F_h(\mathbf{x}) + \Delta F_{micro}(\mathbf{x},\mathbf{y})] \tag{17}$$

In eq 17, $\mathbf{x}$ denotes the cluster distribution so that $\mathbf{x} \equiv \{\phi_s\}$ and $\mathbf{y}$ represents the set of parameters about ordered structure. The superscript ** for ΔF stands for the simultaneous minimization. In ref 15, it is shown that the simultaneous minimization of eq 17 can be approximated by the stepwise minimization of

$$\Delta F_h(\mathbf{x}_o) = \min_{\mathbf{x}} \Delta F_h(\mathbf{x}) \tag{18}$$

$$\Delta F^{**} \cong \min_{\mathbf{y}} G(\mathbf{x}_o,\mathbf{y}) \tag{19}$$

where

$$G(\mathbf{x}_o,\mathbf{y}) = \Delta F_h(\mathbf{x}_o) + \Delta F_{micro}(\mathbf{x}_o,\mathbf{y}) - F_{cor}(\mathbf{x}_o,\mathbf{y}) \tag{20}$$

The correction term F_{cor} in eq 20 accounts for the difference between the simultaneous minimization and the stepwise minimization. We will not reproduce the full derivation of the correction term, which turns out to be

$$F_{cor} = \frac{1}{4!(2\pi)^{12}} \int d\mathbf{q}_1 \int d\mathbf{q}_2 \int d\mathbf{q}_3 \int d\mathbf{q}_4 \Gamma_4^{nl} (\mathbf{q}_1,\mathbf{q}_2,\mathbf{q}_3,\mathbf{q}_4)\Psi(\mathbf{q}_1)\Psi(\mathbf{q}_2)\Psi(\mathbf{q}_3)\Psi(\mathbf{q}_4) \tag{21}$$

Note that the correction term is equal to the nonlocal contribution of the free energy of microstructure and hence they cancel each other in eq 20. In practice, the calculation of the nonlocal term is, therefore, not necessary for the two-step procedure of eqs 18 and 19, and as a result the minimization procedure becomes much simplified. It should be, however, pointed out that the cluster distribution $\mathbf{x}_o$ obtained from eq 18 is not the true cluster distribution that minimizes the total free energy ΔF but is merely the distribution that minimizes the free energy of homogeneous phase ΔF_h. The true cluster distribution $\mathbf{x}^*$ is obtained only by the simultaneous minimization of eq 18. The important point is that the stepwise minimization does not provide the true cluster distribution that minimizes ΔF but does give the minimum of ΔF through a cancellation of an error from eq 18 by the nonlocal term of eq 21.

For the system under study, the cluster distribution is given as $\mathbf{x} = (\phi_1, \phi_2, \phi_{12}, \phi_{121})$. Since the system is assumed to be incompressible, the procedure of eq 18 is expressed as

$$\left[\frac{\partial \Delta F_h}{\partial \phi_{12}}\right]_{\phi_1,\phi_2,\phi_{121},T} = 0, \left[\frac{\partial \Delta F_h}{\partial \phi_{121}}\right]_{\phi_1,\phi_2,\phi_{12},T} = 0 \tag{22}$$

and

$$\phi_1 = \phi - \frac{\phi_{12}}{1+\alpha} - \frac{2\phi_{121}}{2+\alpha}$$

$$\phi_2 = 1 - \phi - \frac{\alpha\phi_{12}}{1+\alpha} - \frac{\alpha\phi_{121}}{2+\alpha} \tag{23}$$

From eqs 2, 22, and 23, the cluster distribution should satisfy

$$\phi_{12} = K_{12}\phi_1\phi_2$$

$$\phi_{121} = K_{121}\phi_1^2\phi_2 \tag{24}$$

The association constants, K_{12} and K_{121} are related to the free energy of a single bonding:

$$K_{12} = \frac{1+\alpha}{N\alpha} \exp\left(-\frac{f_b}{k_B T}\right)$$

$$K_{121} = \frac{2+\alpha}{N^2\alpha} \exp\left(-\frac{2f_b}{k_B T}\right) \tag{25}$$

The free energy of a single bonding, f_b, can be expressed in terms of its energetic and entropic contributions:

$$f_b = \epsilon_b - Ts_b \tag{26}$$

where ϵ_b is the interaction energy of physical bonding and s_b is the entropic loss associated with the formation of a bonding. If we assume that the interaction energy ϵ_b is independent of the temperature, the energy, ϵ_b, can be rewritten as

$$\frac{\epsilon_b}{k_B T} = -\kappa N\chi \tag{27}$$

where κ can be regarded as a molecular parameter describing the interaction of a bonding relative to the degree of incompatibility in A/B blends ($N\chi$) and thus characterizes the competition between two opposite interactions, i.e., favorable bonding energy between functionalized monomers and unfavorable dispersive interaction between A- and B-monomers ($\kappa > 0$). Furthermore, the entropic part s_b is expressed in terms of the relative orientations of functionalized monomers in a bonding

$$s_b = -k_B \ln(q/N) \tag{28}$$

where q is the number of relative orientations for a pair of functionalized monomer in contact. The additional

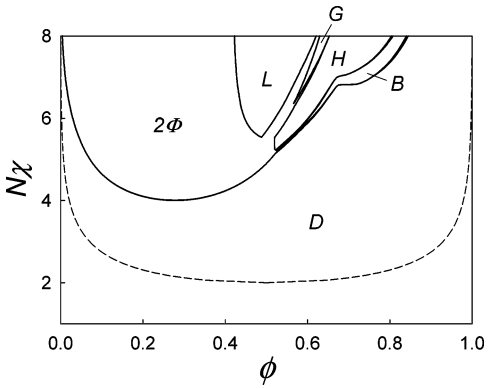

Figure 2. Phase diagram of mono-end-functionalized A-chain/di-end-functionalized B-chain for $\{\alpha = 1.0, \kappa = 2.0, q_{eff} = 100\}$. The dashed line represents the binodal curve of the corresponding blend without functionalized monomer.

term of $k_B \ln N$ accounts for the spatial localization of a functionalized end-segment having Kuhnian length $l_k \sim N^{-1}$ in contact with its functional pair. The free energy change of homogeneous phase in eq 1 is then rewritten as

$$\frac{N\Delta F_h}{Vk_BT} = \left(\frac{\phi_{12}}{1+\alpha} + \frac{2\phi_{121}}{2+\alpha}\right)(1 - \kappa N\chi + \ln q_{eff}) + \frac{\phi_{12}}{1+\alpha}\ln\frac{\alpha}{1+\alpha} + \frac{\phi_{121}}{2+\alpha}\ln\frac{\alpha}{2+\alpha} + \phi_1 \ln \phi_1 + \frac{\phi_2}{\alpha}\ln \phi_{21} + \frac{\phi_{12}}{1+\alpha}\ln \phi_{12} + \frac{\phi_{121}}{2+\alpha}\ln \phi_{121} + N\chi\phi(1-\phi) \quad (29)$$

where $q_{eff} = q/(z-1)$. For hydrogen bond, the bonding energy lies in the range 1−10 kcal/mol and the magnitude of the entropic change is the order of 10 cal/(K·mol), which roughly corresponds to $\kappa/N \approx 100$ and $q_{eff} \approx 100$.[24,25]

For a given set of molecular parameters $\{\alpha, \kappa, q\}$, the phase diagram in the $(N\chi, \phi)$ plane is constructed as follow. First, the cluster distribution satisfying eq 18, $\mathbf{x}_o = (\tilde{\phi}_1, \tilde{\phi}_2, \tilde{\phi}_{12}, \tilde{\phi}_{121})$, is obtained as a function of $N\chi$ and ϕ by solving eqs 23 and 24. Second, the total free energy without nonlocal term, $G(\mathbf{x}_o,\mathbf{y})$, is expressed by inserting $\mathbf{x}_o = (\tilde{\phi}_1, \tilde{\phi}_2, \tilde{\phi}_{12}, \tilde{\phi}_{121})$ into eq 20, and then ΔF^{**} is obtained by minimizing $G(\mathbf{x}_o,\mathbf{y})$ with respect to the parameters describing ordered structure $\mathbf{y}$. Finally, the phase coexistence curve is determined by the common tangent construction of

$$\left.\frac{\partial \Delta F^{**}}{\partial \phi}\right|_{\phi'} = \left.\frac{\partial \Delta F^{**}}{\partial \phi}\right|_{\phi''} = \mu$$

$$\Delta F^{**}(\phi') - \mu\phi' = \Delta F^{**}(\phi'') - \mu\phi'' \quad (30)$$

where ϕ' and ϕ'' are the compositions of the coexisting phases.

Using the theoretical formulations described above, the phase diagrams of binary blends of mono-end-functionalized A-chain and di-end-functionalized B-chain are obtained and presented in the next section. For the association parameters of $\{\kappa, q_{eff}\}$, we restrict ourselves to one set of values of $\{\kappa = 2, q_{eff} = 100\}$, which roughly corresponds to the parameters for a hydrogen bonding between end-functionalized polymers having the degree of polymerization, $N \approx 100$.

III. Results and Discussions

Figure 2 presents the phase diagram of binary blends

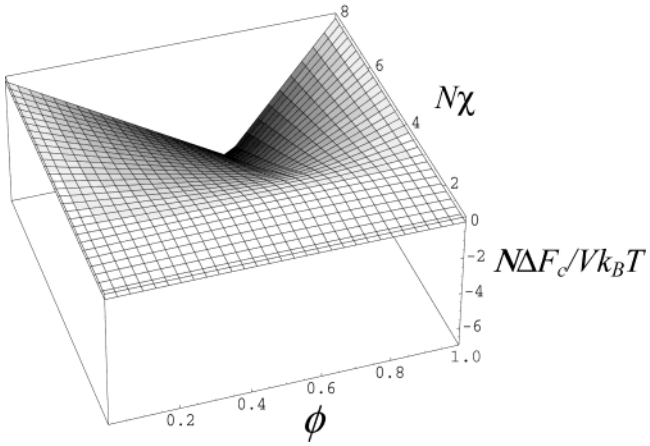

Figure 3. Free energy of clustering, ΔF_c, as a function of $N\chi$ and ϕ for $\{\alpha = 1.0, \kappa = 2.0, q = 100\}$.

of mono-end-functionalized A-chain and di-end-functionalized B-chain for the set of molecular parameters of $\{\alpha = 1, \kappa = 2, q_{eff} = 100\}$. For comparison, the phase diagram of the blend without functionalized monomers is also shown by dashes line. In the diagram, the alphabetic letters indicate the type of structures: (D) disordered; (L) lamellar; (G) double gyroid; (H) hexagonal; (B) body-centered cubic. The "2Φ" represents the biphasic coexistence between two different structures. Figure 2 shows that most of ordered structures are found in the region $0.5 < \phi < 0.7$ whereas the biphasic regions dominate at $\phi < 0.5$. This can be understood as follows. In the blend shown in Figure 2, where the A- and the B-chain have an equal degree of polymerization of N ($\alpha = 1$), the magnitude of the free energy contribution due to the clustering between A- and B-chains is maximized at the stoichiometric composition $\phi_{st} = 2/(2 + \alpha) = {}^2/_3$. This is illustrated in Figure 3 where the free energy contribution due to the clustering ΔF_c is plotted against $N\chi$ and ϕ. The free energy contribution due to clustering ΔF_c is given as

$$\frac{N\Delta F_c}{Vk_BT} = \left(\frac{\phi_{12}}{1+\alpha} + \frac{2\phi_{121}}{2+\alpha}\right)(1 - \kappa N\chi + \ln q_{eff}) \quad (31)$$

Clustering between A- and B-chains due to the formation of bonds competes with the segregation between A- and B-monomer. The latter becomes the maximum at $\phi = {}^1/_2$ when $N\chi$ is not too small, since the energy contribution due to unfavorable AB contacts is proportional to $\phi(1-\phi)$. In the region ${}^1/_2 < \phi < {}^2/_3$ and large $N\chi$, these two competing interactions are balanced by forming a microphase separation between A-chains and B-chains with most of their end-functional pairs attached to each other. Therefore, most of ordered structures are found in the region ${}^1/_2 < \phi < {}^2/_3$ where two effects strongly competes with each other. On the other hand, in the region $\phi \ll {}^2/_3$ where the blend contains a larger fraction of unpaired B-chains, the unpaired B-chains segregate from the clusters as $N\chi$ increases, leading to a biphasic coexistence between a disordered phase with a large amount of free B-chains, and a cluster-rich phase of disordered or ordered structure. Conversely, in the region $\phi > {}^2/_3$ where the blend contains a relatively small fraction of unpaired A-chains, the clustering dominates the segregation, and thereby, relatively larger regions remain as a disordered phase.

Another feature in the phase diagram of Figure 2 is that the regions of ordered structures (L, G, H, B) are

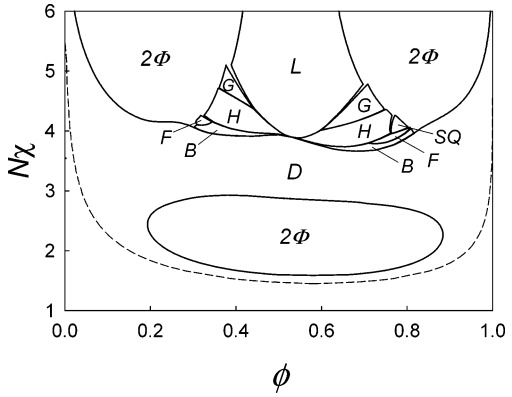

Figure 4. Phase diagram of mono-end-functionalized A-chain/di-end-functionalized B-chain for $\{\alpha = 2.0, \kappa = 2.0, q_{eff} = 100\}$. The dashed line represents the binodal curve of the corresponding blend without functionalized monomer.

separated from each other by narrow regions of biphasic coexistence between two different ordered structures (L + G, L + H, G + H, H + B). This is explained by the following example. Suppose that there is an order−order transition point ϕ_{tr} at which the total free energy of an ordered phase (for instance the L phase) is equal to that of another type of ordered phase (for instance the G phase). In such a case, the free energy derivative $\partial\Delta F/\partial\phi$ of the L phase should be smaller or larger than that of the G phase at either side of ϕ_{tr}, since otherwise it would not be possible to have ϕ_{tr}. Therefore, the ΔF has a cusp in the narrow region around ϕ_{tr}, leading to a biphasic coexistence between two different ordered phases, instead of having the order−order transition at ϕ_{tr}.

The phase diagram of Figure 2 was obtained for the case of symmetric blends in which A-chain and B-chain have an equal degree of polymerization ($\alpha = 1$). We now consider the asymmetric case of $\alpha > 1$, i.e., where the degree of polymerization of the B-chain is larger than that of the A-chain. When the phase diagram of an asymmetric blend with $\{\alpha = 2, \kappa = 2, q = 100\}$ is drawn on the plane of $N\chi$ vs ϕ, as shown in Figure 4, the blends are macrophase-separated at the moderate value of $N\chi = 1.6-3$ by forming a biphasic coexistence between two disordered states. This biphasic coexistence disappears and the mixture is rehomogenized for $N\chi = 3-4$ where the tendency of association ($\kappa N\chi$) becomes strong enough to create more clusters that act as compatibilizers for the mixture. This sequence of phase behavior, i.e., the upper critical temperature ($N\chi \cong 1.6$) and the lower critical temperature ($N\chi \cong 3$), produces a "closed loop" phase diagram, which is one of the characteristics of the phase behavior observed in the mixtures involving specific interactions.[26,27] Note that the loop is flatter near the lower critical temperature ($N\chi \cong 3$) than the upper critical temperature ($N\chi \cong 1.6$). This can be explained by the following. Since copolymer-like clusters become predominantly prevailing due to the bond formation between end-functionalized monomers at $N\chi > 3$, the entropy of the system becomes very low due to the directional specific nature of end-association that is characterized by $q \gg 1$ (in our work, $q_{eff} = q/(z - 1) = 100$). On the other hand, the mixture is macroscopically phase-separated inside loop where most of homopolymers remain free. Because the change of the system entropy is not drastic as $N\chi$ increases, the only way for the phase-separated mixture to have a small entropy is to reduce its configurational entropy, which is achieved by a wide separation between two binodal

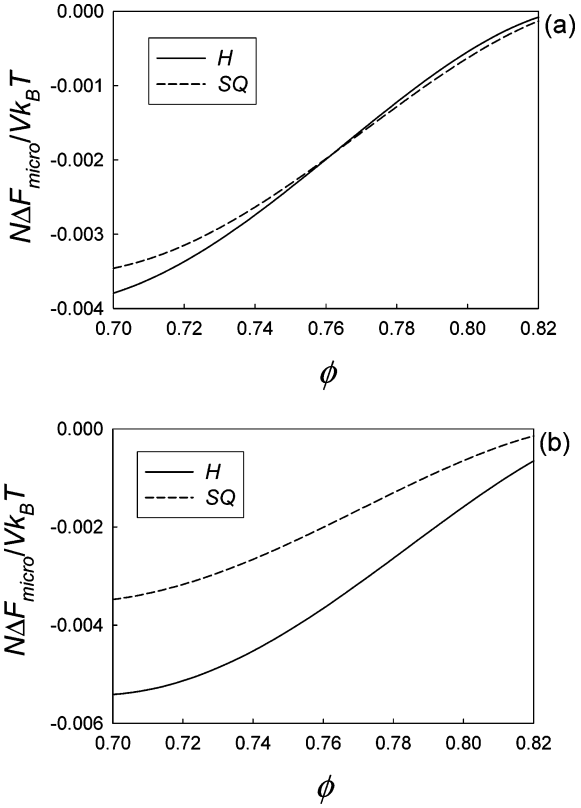

Figure 5. Free energy of microstructure for the H phase and the SQ phase plotted as a function of ϕ at $N\chi = 4.1$ for $\{\alpha = 2.0, \kappa = 2.0, q_{eff} = 100\}$: (a) when the wave vector cutoff criterion is $Q \le 2^{1/2}Q_1$; (b) when the wave vector cutoff criterion is $Q \le 2Q_1$.

points (ϕ', ϕ'') near $N\chi \cong 3$.

When $N\chi$ becomes even larger than $N\chi = 4$, various types of ordered structures (L, G, H, B, F, SQ) are observed at the regions around the stoichiometric composition $\phi_{st} = 1/2$ and their regions are separated by the biphasic regions. The most notable feature in the regime of $N\chi > 4$ is the stable region of the cylindrical phase arranged with square symmetry (SQ) at the region of $\phi \approx 0.76-0.79$ and $N\chi \approx 3.8-4.2$. This is a very surprising result since, to our knowledge, the SQ phase has never been reported to be a stable phase in any specific system consisting of A- and B-monomers. A decade ago, Marques and Cates speculated that the SQ phase could be stable in addition to the classical phase.[28] However, they only predicted the criteria of the coefficients, Γ_2, Γ_3, and Γ_4, for a stable SQ phase and therefore could not indicate which specific system could show the morphology of the SQ phase.

It should be, however, remembered that our calculation for the stability of the SQ phase is based on the harmonic approximation with the cutoff criterion of $Q \le 2^{1/2}Q_1$. It is well-known that the value of the Landau free energy depends in a sensitive way on the number of harmonics used in the calculation. Therefore, it is important to make sure that the cutoff criterion used for the harmonic contribution to the Landau free energy gives a reasonable accuracy. To examine if the SQ phase is truly stable in the indicated region shown in Figure 4, we have performed an additional calculation for the harmonic contribution using the criteria extended to $Q \le 2Q_1$, which corresponds to a third harmonics calculation for the SQ phase. In Figure 5, the values of Landau free energies for SQ and H phases calculated with two

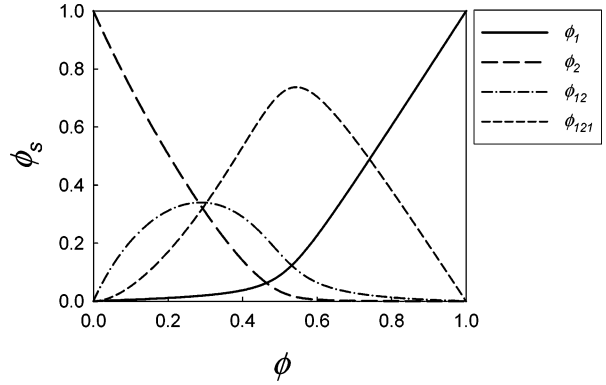

Figure 6. Cluster distribution $\tilde{\phi}_s(s = 1/2/12/121)$ plotted as a function of ϕ at $N\chi = 4.1$ for $\{\alpha = 2.0, \kappa = 2.0, q_{\text{eff}} = 100\}$.

different cutoff criteria of $Q \leq 2^{1/2}Q_1$ (Figure 5a) and $Q \leq 2Q_1$ (Figure 5b) are plotted against ϕ for $N\chi = 4.1$ where the SQ phase is found to be stable at $\phi = 0.76-0.80$ in the phase diagram shown in Figure 4. Figure 5 shows that the SQ phase becomes unstable against the H phase when the cutoff criterion is extended to $Q \leq 2Q_1$, while it is stable at $\phi = 0.76-0.80$ according to the criterion of $Q \leq 2^{1/2}Q_1$. When the phase diagram (not shown here) based on the harmonics approximation with $Q \leq 2Q_1$ is compared with that (Figure 4) based on the harmonics approximation with $Q \leq 2^{1/2}Q_1$, it reveals that the two phase diagram are nearly the same except the existence of the SQ phase in Figure 4 which is replaced by mostly that of the H phase in the phase diagram base on $Q \leq 2Q_1$. The conflicting result with respect to the stability of SQ phase is very much concerned with exclusion of the second harmonic contribution for the H phase ($Q_2 = 3^{1/2}Q_1$) when the criterion $Q \leq 2^{1/2}Q_1$ is used for the free energy calculation. When Figure 5a is compared to Figure 5b, it is obvious that the contribution of higher harmonics for H phase is nontrivial particularly in the region of large $|\phi - \phi_{\text{st}}|$ where the system contains many unpaired, free A-chains. In such regions, the situation is very similar to the case when a large amount of homopolymers are added to block copolymers, and thus the period of the ordered phase is much larger than the size of a minor domain formed by associated B-homopolymers since a large excess of free A-homopolymers is filled in the matrix of the ordered phase, producing a density profile which may be very different from sinusoidal. In such a case, many harmonic contributions should be included to calculate the Landau free energy with reasonable accuracy since only a single harmonic cannot represents the density profiles of such swollen phase. Therefore, the exclusion of the contribution of harmonics higher than the first harmonics for the H phase makes the free energy calculation less accurate particularly when $|\phi - \phi_{\text{st}}|$ is large. For this reason, we must conclude that the stable SQ phase in the phase diagram shown in Figure 4 is an artifact due to the wave vector cutoff criterion of $Q \leq 2^{1/2}Q_1$ used in this study. On the basis of the new calculation with the cutoff criterion of $Q \leq 2Q_1$, the region of the SQ phase in Figure 4 should be replaced by the H phase.

However, it should be noted that as shown in Figure 5, the relative stability of SQ phase against the H phase is enhanced when ϕ increases although the SQ phase does not completely dominate over the H phase. As shown in Figure 6, the situation in the region $\phi > 0.5$ and $N\chi = 4.1$ is very similar to the case when a large

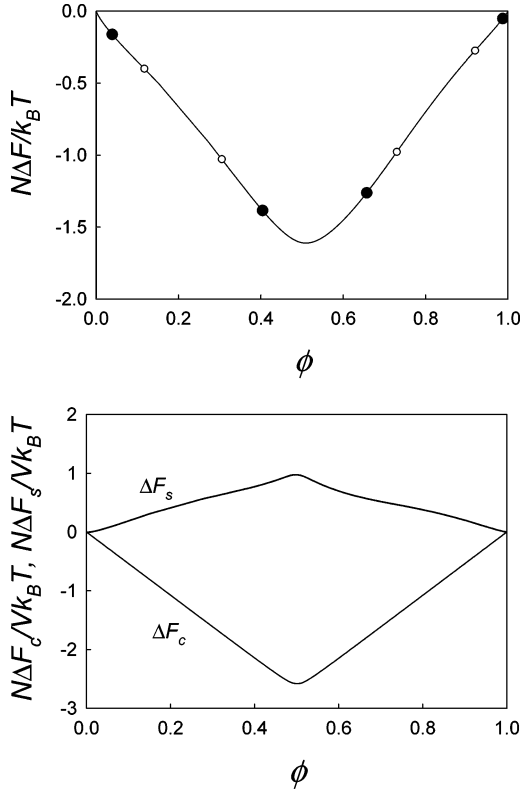

Figure 7. Free energy plotted as a function of ϕ at $N\chi = 5.5$ for $\{\alpha = 2.0, \kappa = 2.0, q_{\text{eff}} = 100\}$: (a) the total free energy ΔF; (b) the free energy contribution of clustering ΔF_c and the free energy contribution of segregation $\Delta F_s = \Delta F - \Delta F_c$. The filled and open circles in part a represent the binodal points and the spinodal points, respectively.

amount of A-homopolymers with the degree of polymerization of $2N$ are added to the ABA triblock copolymers with the degree of polymerization of $4N$. It is known that the addition of homopolymers to block copolymers stabilizes morphologies that are unstable in the pure block copolymer melt. For instance, Matsen[29] has predicted that a G phase transforms to a HPL phase on addition of homopolymer to the matrix phase of block copolymer. This is due to the fact that the addition of homopolymer to the matrix phase relieves packing frustration of the majority block which has to fill the space of the matrix phase possessing nonuniform curvature of the interface. A similar interpretation can be applied to the relative phase stability between the H phase and the SQ phase. Since the interfacial area per unit volume for the square arrangement of cylinders is smaller than that for the hexagonally packed cylinders, the SQ phase is energetically more favorable than the H phase. On the other hand, the packing frustration of A-chains of AB or ABA blocklike clusters in the matrix is more severe for the SQ phase than that for the H phase, since some of the A-chains bonded with the B-chains should be more stretched in order to fill the corner of the Wigner−Seitz cell of the square lattice. Such an entropic penalty imposed on the associated triblocklike clusters is much relieved by the presence of free A-chains, a large portion of which can be, located at the corners of the Wigner−Seitz cell. Therefore, the enhancement of the stability for the SQ phase relative to the H phase can be explained by the relief of packing frustration by free homopolymers.

Another feature in Figure 4 to note is that, apart from the relatively narrow biphasic regions between two

different ordered structures, the phase coexistence between a D phase and an ordered phase dominates the phase diagram in the region of $\phi < 0.5$ and $\phi > 0.5$ when $N\chi$ is large. As seen in Figure 7a which presents the total free energy curve at $N\chi = 5.5$, the total free energy shows two convex regions at $\phi < 0.5$ and $\phi > 0.5$. This is because the free energy contribution of clustering asymptotically approaches $\Delta F_c \sim f_b|\phi - \phi_{st}|$ whereas the free energy contribution due to the segregation ($\Delta F_s = \Delta F - \Delta F_c$) becomes highly convex shape when $N\chi$ is large (Figure 7b). These two competing tendencies yield the convex regions at both regions of $\phi < 0.5$ and $\phi > 0.5$ in the $\Delta F - \phi$ curve, leading to the phase coexistence between the D phase and the ordered phases. The latter effect counters the localization of free chains in the matrix phase of an ordered structure and, therefore, prevents the formation of ordered structures with highly swollen matrix domains when $|\phi - \phi_{st}|$ is large.

IV. Summary

In this paper, we have theoretically calculated the phase diagram for the blend of mono-end-functionalized polymer and di-end-functionalized polymer, which are capable of forming triblocklike supramolecules. The predicted phase diagrams show that various types of ordered structures can be formed at the region around the stoichiometric composition as a result of competition between clustering and segregation. Furthermore, our results show that under a specific condition these associating blend systems can have both of the upper critical temperature and the lower critical temperature, producing a "closed loop" phase diagram, which is one of the characteristics of the phase behavior observed in the mixtures involving specific interactions.

It is also found that in all the blend systems under our consideration, the cylindrical phase arranged in square symmetry is always unstable against hexagonally arranged cylindrical phase according to the harmonic corrections up to the third harmonics. Nevertheless, our results do not rule out a possible stabilization of square phase by an addition of homopolymer to the matrix phase of block copolymer which may be found in other systems although the present system under study is not the case of systems with stable square phase.

Acknowledgment. J.H. thanks the Ministry of Education, the Republic of Korea, for their financial support through the BK21 program.

Appendix A: Correlation Function, $\bar{g}$

The correlation function $\bar{g}$ for the system under consideration is given from eq 9:

$$\bar{g}_{ij\cdots} = \frac{\tilde{\phi}_1}{N} g^{(1)}_{ij\cdots} + \frac{\tilde{\phi}_2}{N\alpha} g^{(2)}_{ij\cdots} + \frac{\tilde{\phi}_{12}}{N(1+\alpha)} g^{(12)}_{ij\cdots} + \frac{\tilde{\phi}_{121}}{N(2+\alpha)} g^{(121)}_{ij\cdots} \quad \text{(A1)}$$

where $g^{(s)}_{ij\cdots}$ is the monomer density correlation functions of a single cluster or chain of type s. The cluster distribution $\{\tilde{\phi}_1, \tilde{\phi}_2, \tilde{\phi}_{12}, \tilde{\phi}_{121}\}$ is given from eqs 23 and 24. Using eq A1, the nth order single chain correlation functions are given as follows.

The second-order density correlation functions $\bar{g}_{\alpha\beta}$ are given by

$$\bar{g}_{AA}(x) = \frac{2N\psi_1}{x^2}(x + e^{-x} - 1) + \frac{2N\psi_2}{x^2} e^{-x\alpha}(1 - e^{-x})^2 \quad \text{(A2)}$$

$$\bar{g}_{BB}(x) = \frac{2N\psi_3}{x^2}(x\alpha + e^{-x\alpha} - 1) \quad \text{(A3)}$$

$$\bar{g}_{AB}(x) = \frac{N\psi_4}{x^2}(1 - e^{-x})(1 - e^{-x\alpha}) \quad \text{(A4)}$$

Here $x = |\mathbf{q}_1|^2 R^2$ where R is the radius of gyration of an ideal chain of N monomers, and

$$\psi_1 = \tilde{\phi}_1 + \frac{\tilde{\phi}_{12}}{1+\alpha} + \frac{2\tilde{\phi}_{121}}{2+\alpha}, \quad \psi_2 = \frac{\tilde{\phi}_{121}}{2+\alpha}$$
$$\psi_3 = \frac{\tilde{\phi}_2}{\alpha} + \frac{\tilde{\phi}_{12}}{1+\alpha} + \frac{\tilde{\phi}_{121}}{2+\alpha}, \quad \psi_4 = \frac{\tilde{\phi}_{12}}{1+\alpha} + \frac{2\tilde{\phi}_{121}}{2+\alpha} \quad \text{(A5)}$$

For the third-order correlation functions, the following function is introduced:

$$\bar{g}_{\alpha\beta\gamma}(\mathbf{q}_1, \mathbf{q}_2, \mathbf{q}_3) = \bar{g}_{\alpha\beta\gamma}(x, \eta_2, \eta_3) \quad \text{(A6)}$$

where η_i is defined as $\eta_i = |\mathbf{q}_i|^2/|\mathbf{q}_1|^2$. The $\mathbf{q}$ dependence of $\bar{g}_{\alpha\beta\gamma}$ is taken into account only by η_i's since $\mathbf{q}_1 + \mathbf{q}_2 + \mathbf{q}_3 = 0$. Following the notation above, the third-order correlation functions $\bar{g}_{\alpha\beta\gamma}$ are

$$\bar{g}_{AAA}(x,\eta_2,\eta_3) = 2N^2\psi_1[f_1(x,1,\eta_2,1) + f_1(x,1,1,\eta_3) + f_1(x,1,\eta_2,\eta_3)] + 2N^2\psi_2[f_2(x,1,1,\eta_2) + f_2(x,1,1,\eta_3) + f_2(x,1,\eta_2,1) + f_2(x,1,\eta_3,1) + f_2(x,1,\eta_2,\eta_3) + f_2(x,1,\eta_3,\eta_2)] \quad \text{(A7)}$$

$$\bar{g}_{BBB}(x,\eta_2,\eta_3) = 2N^2\psi_3[f_1(x,\alpha,\eta_2,1) + f_1(x,\alpha,1,\eta_3) + f_1(x,\alpha,\eta_2,\eta_3)] \quad \text{(A8)}$$

$$\bar{g}_{AAB}(x,\eta_2,\eta_3) = N^2\psi_4[f_3(x,\alpha,1,\eta_3) + f_3(x,\alpha,\eta_2,\eta_3)] + 2N^2\psi_2 f_4(x,\alpha,\eta_2,1) \quad \text{(A9)}$$

$$\bar{g}_{BBA}(x,\eta_2,\eta_3) = N^2\psi_4[f_5(x,\alpha,1,\eta_3) + f_5(x,\alpha,\eta_2,\eta_3)] \quad \text{(A10)}$$

$$\bar{g}_{ABA}(x,\eta_2,\eta_3) = N^2\psi_4[f_3(x,\alpha,1,\eta_2) + f_3(x,\alpha,\eta_3,\eta_2)] + 2N^2\psi_2 f_4(x,\alpha,1,\eta_3) \quad \text{(A11)}$$

$$\bar{g}_{BAB}(x,\eta_2,\eta_3) = N^2\psi_4[f_5(x,\alpha,1,\eta_2) + f_5(x,\alpha,\eta_3,\eta_2)] \quad \text{(A12)}$$

$$\bar{g}_{BAA}(x,\eta_2,\eta_3) = N^2\psi_4[f_3(x,\alpha,\eta_2,1) + f_3(x,\alpha,\eta_3,1)] + 2N^2\psi_2 f_4(x,\alpha,\eta_2,\eta_3) \quad \text{(A13)}$$

where

$$f_1(x,\alpha,m,n) = \int_0^{\alpha} \mathrm{d}i \int_0^{i} \mathrm{d}j \int_0^{j} \mathrm{d}k\ \mathrm{e}^{-mx(j-k)}\mathrm{e}^{-nx(i-j)} \quad \text{(A14)}$$

$$f_2(x,\alpha,m,n) = \int_0^{1} \mathrm{d}i \int_i^{1} \mathrm{d}j \int_{1+\alpha}^{2+\alpha} \mathrm{d}k\ \mathrm{e}^{-mx(j-i)}\mathrm{e}^{-nx(k-j)} \quad \text{(A15)}$$

$$f_3(x,\alpha,m,n) = \int_0^{1} \mathrm{d}i \int_i^{1} \mathrm{d}j \int_{1}^{1+\alpha} \mathrm{d}k\ \mathrm{e}^{-mx(j-i)}\mathrm{e}^{-nx(k-j)} \quad \text{(A16)}$$

$$f_4(x,\alpha,m,n) = \int_0^{1} \mathrm{d}i \int_1^{1+\alpha} \mathrm{d}j \int_{1+\alpha}^{2+\alpha} \mathrm{d}k\ \mathrm{e}^{-mx(j-i)}\mathrm{e}^{-nx(k-j)} \quad \text{(A17)}$$

$$f_5(x,\alpha,m,n) = \int_1^{1+\alpha} \mathrm{d}i \int_1^{i} \mathrm{d}j \int_0^{1} \mathrm{d}k\ \mathrm{e}^{-mx(i-j)}\mathrm{e}^{-nx(j-k)} \quad \text{(A18)}$$

Similarly, the following function is used for the fourth order correlation function:

$$\bar{g}_{\alpha}\beta\gamma\delta(\mathbf{q}_1,\mathbf{q}_2,\mathbf{q}_3,\mathbf{q}_4) = \bar{g}_{\alpha\beta\gamma\delta}(x,\eta_2,\eta_3,\eta_4,h_2,h_3,h_4) \quad \text{(A19)}$$

where h_i is defined by $h_i = |\mathbf{q}_1 + \mathbf{q}_i|^2/|\mathbf{q}_1|^2$and accounts for the angular dependence of $\bar{g}_{\alpha\beta\gamma\delta}(\mathbf{q}_1,\mathbf{q}_2,\mathbf{q}_3,\mathbf{q}_4)$. The fourth order correlation functions $\bar{g}_{\alpha\beta\gamma\delta}$ are then expressed as

$$\bar{g}_{\mathrm{AAAA}}(x,\eta_2,\eta_3,\eta_4,h_2,h_3,h_4) = 2N^3\psi_1[f_6(x,1,h_2,1,\eta_3) + f_6(x,1,h_2,1,\eta_4) + f_6(x,1,h_2,\eta_2,\eta_3) + f_6(x,1,h_2,\eta_2,\eta_4) + f_6(x,1,h_3,1,\eta_2) + f_6(x,1,h_3,1,\eta_4) + f_6(x,1,h_3,\eta_3,\eta_2) + f_6(x,1,h_3,\eta_3,\eta_4) + f_6(x,1,h_4,1,\eta_2) + f_6(x,1,h_4,1,\eta_3) + f_6(x,1,h_4,\eta_4,\eta_2) + f_6(x,1,h_4,\eta_4,\eta_3)] + 2N^3\psi_2[f_7(x,\alpha,h_2,1,\eta_3) + f_7(x,\alpha,h_2,1,\eta_4) + f_7(x,\alpha,h_2,\eta_2,\eta_3) + f_7(x,\alpha,h_2,\eta_2,\eta_4) + f_7(x,\alpha,h_3,1,\eta_2) + f_7(x,\alpha,h_3,1,\eta_4) + f_7(x,\alpha,h_3,\eta_3,\eta_2) + f_7(x,\alpha,h_3,\eta_3,\eta_4) + f_7(x,\alpha,h_4,1,\eta_2) + f_7(x,\alpha,h_4,1,\eta_3) + f_7(x,\alpha,h_4,\eta_4,\eta_2) + f_7(x,\alpha,h_4,\eta_4,\eta_3) + f_7(x,\alpha,h_2,\eta_3,1) + f_7(x,\alpha,h_2,\eta_4,1) + f_7(x,\alpha,h_2,\eta_3,\eta_2) + f_7(x,\alpha,h_2,\eta_4,\eta_2) + f_7(x,\alpha,h_3,\eta_2,1) + f_7(x,\alpha,h_3,\eta_4,1) + f_7(x,\alpha,h_3,\eta_2,\eta_3) + f_7(x,\alpha,h_3,\eta_4,\eta_3) + f_7(x,\alpha,h_4,\eta_2,1) + f_7(x,\alpha,h_4,\eta_3,1) + f_7(x,\alpha,h_4,\eta_2,\eta_4) + f_7(x,\alpha,h_4,\eta_3,\eta_4) + f_8(x,\alpha,h_2,1,\eta_3) + f_8(x,\alpha,h_2,1,\eta_4) + f_8(x,\alpha,h_2,\eta_2,\eta_3) + f_8(x,\alpha,h_2,\eta_2,\eta_4) + f_8(x,\alpha,h_3,1,\eta_2) + f_8(x,\alpha,h_3,1,\eta_4) + f_8(x,\alpha,h_3,\eta_3,\eta_2) + f_8(x,\alpha,h_3,\eta_3,\eta_4) + f_8(x,\alpha,h_4,1,\eta_2) + f_8(x,\alpha,h_4,1,\eta_3) + f_8(x,\alpha,h_4,\eta_4,\eta_2) + f_8(x,\alpha,h_4,\eta_4,\eta_3)] \quad \text{(A20)}$$

$$\bar{g}_{\mathrm{BBBB}}(x,\eta_2,\eta_3,\eta_4,h_2,h_3,h_4) = 2N^3\psi_3[f_6(x,\alpha,h_2,1,\eta_3) + f_6(x,\alpha,h_2,1,\eta_4) + f_6(x,\alpha,h_2,\eta_2,\eta_3) + f_6(x,\alpha,h_2,\eta_2,\eta_4) + f_6(x,\alpha,h_3,1,\eta_2) + f_6(x,\alpha,h_3,1,\eta_4) + f_6(x,\alpha,h_3,\eta_3,\eta_2) + f_6(x,\alpha,h_3,\eta_3,\eta_4) + f_6(x,\alpha,h_4,1,\eta_2) + f_6(x,\alpha,h_4,1,\eta_3) + f_6(x,\alpha,h_4,\eta_4,\eta_2) + f_6(x,\alpha,h_4,\eta_4,\eta_3)] \quad \text{(A21)}$$

$$\bar{g}_{\mathrm{AAAB}}(x,\eta_2,\eta_3,\eta_4,h_2,h_3,h_4) = N^3\psi_4[f_9(x,\alpha,h_2,1,\eta_4) + f_9(x,\alpha,h_2,\eta_2,\eta_4) + f_9(x,\alpha,h_3,1,\eta_4) + f_9(x,\alpha,h_3,\eta_3,\eta_4) + f_9(x,\alpha,h_4,\eta_2,\eta_4) + f_9(x,\alpha,h_4,\eta_3,\eta_4)] + 2N^3\psi_2[f_{10} \times (x,\alpha,h_2,1,\eta_3) + f_{10}(x,\alpha,h_2,\eta_2,\eta_3) + f_{10}(x,\alpha,h_3,1,\eta_2) + f_{10}(x,\alpha,h_3,\eta_3,\eta_2) + f_{10}(x,\alpha,h_4,\eta_2,1) + f_{10}(x,\alpha,h_4,\eta_3,1)] \quad \text{(A22)}$$

$$\bar{g}_{\mathrm{BBBA}}(x,\eta_2,\eta_3,\eta_4,h_2,h_3,h_4) = N^3\psi_4[f_{11}(x,\alpha,h_2,1,\eta_4) + f_{11}(x,\alpha,h_2,\eta_2,\eta_4) + f_{11}(x,\alpha,h_3,1,\eta_4) + f_{11}(x,\alpha,h_3,\eta_3,\eta_4) + f_{11}(x,\alpha,h_4,\eta_2,\eta_4) + f_{11}(x,\alpha,h_4,\eta_3,\eta_4)] \quad \text{(A23)}$$

$$\bar{g}_{\mathrm{AABA}}(x,\eta_2,\eta_3,\eta_4,h_2,h_3,h_4) = N^3\psi_4[f_9(x,\alpha,h_2,1,\eta_3) + f_9(x,\alpha,h_2,\eta_2,\eta_3) + f_9(x,\alpha,h_3,\eta_2,\eta_3) + f_9(x,\alpha,h_3,\eta_4,\eta_3) + f_9(x,\alpha,h_4,1,\eta_3) + f_9(x,\alpha,h_4,\eta_4,\eta_3)] + 2N^3\psi_2[f_{10} \times (x,\alpha,h_2,1,\eta_4) + f_{10}(x,\alpha,h_2,\eta_2,\eta_4) + f_{10}(x,\alpha,h_3,\eta_4,1) + f_{10}(x,\alpha,h_3,\eta_2,1) + f_{10}(x,\alpha,h_4,1,\eta_2) + f_{10}(x,\alpha,h_4,\eta_4,\eta_2)] \quad \text{(A24)}$$

$$\bar{g}_{\mathrm{BBAB}}(x,\eta_2,\eta_3,\eta_4,h_2,h_3,h_4) = N^3\psi_4[f_{11}(x,\alpha,h_2,1,\eta_3) + f_{11}(x,\alpha,h_2,\eta_2,\eta_3) + f_{11}(x,\alpha,h_3,\eta_2,\eta_3) + f_{11}(x,\alpha,h_3,\eta_4,\eta_3) + f_{11}(x,\alpha,h_4,1,\eta_3) + f_{11}(x,\alpha,h_4,\eta_4,\eta_3)] \quad \text{(A25)}$$

$$\bar{g}_{\mathrm{ABAA}}(x,\eta_2,\eta_3,\eta_4,h_2,h_3,h_4) = N^3\psi_4[f_9(x,\alpha,h_2,\eta_3,\eta_2) + f_9(x,\alpha,h_2,\eta_4,\eta_2) + f_9(x,\alpha,h_3,1,\eta_2) + f_9(x,\alpha,h_3,\eta_3,\eta_2) + f_9(x,\alpha,h_4,1,\eta_2) + f_9(x,\alpha,h_4,\eta_4,\eta_2)] + 2N^3\psi_2[f_{10} \times (x,\alpha,h_2,\eta_4,1) + f_{10}(x,\alpha,h_2,\eta_3,1) + f_{10}(x,\alpha,h_3,1,\eta_4) + f_{10}(x,\alpha,h_3,\eta_3,\eta_4) + f_{10}(x,\alpha,h_4,1,\eta_3) + f_{10}(x,\alpha,h_4,\eta_4,\eta_3)] \quad \text{(A26)}$$

$$\bar{g}_{\mathrm{BABB}}(x,\eta_2,\eta_3,\eta_4,h_2,h_3,h_4) = N^3\psi_4[f_{11}(x,\alpha,h_2,\eta_3,\eta_2) + f_{11}(x,\alpha,h_2,\eta_4,\eta_2) + f_{11}(x,\alpha,h_3,1,\eta_2) + f_{11}(x,\alpha,h_3,\eta_3,\eta_2) + f_{11}(x,\alpha,h_4,1,\eta_2) + f_{11}(x,\alpha,h_4,\eta_4,\eta_2)] \quad \text{(A27)}$$

$$\bar{g}_{\mathrm{BAAA}}(x,\eta_2,\eta_3,\eta_4,h_2,h_3,h_4) = N^3\psi_4[f_9(x,\alpha,h_2,\eta_3,1) + f_9(x,\alpha,h_2,\eta_4,1) + f_9(x,\alpha,h_3,\eta_2,1) + f_9(x,\alpha,h_3,\eta_4,1) + f_9(x,\alpha,h_4,\eta_3,1) + f_9(x,\alpha,h_4,\eta_2,1)] + 2N^3\psi_2[f_{10} \times (x,\alpha,h_2,\eta_3,\eta_2) + f_{10}(x,\alpha,h_2,\eta_4,\eta_2) + f_{10}(x,\alpha,h_3,\eta_4,\eta_3) + f_{10}(x,\alpha,h_3,\eta_2,\eta_3) + f_{10}(x,\alpha,h_4,\eta_3,\eta_4) + f_{10}(x,\alpha,h_4,\eta_2,\eta_4)] \quad \text{(A28)}$$

$$\bar{g}_{\mathrm{ABBB}}(x,\eta_2,\eta_3,\eta_4,h_2,h_3,h_4) = N^3\psi_4[f_{11}(x,\alpha,h_2,\eta_3,1) + f_{11}(x,\alpha,h_2,\eta_4,1) + f_{11}(x,\alpha,h_3,\eta_2,1) + f_{11}(x,\alpha,h_3,\eta_4,1) + f_{11}(x,\alpha,h_4,\eta_3,1) + f_{11}(x,\alpha,h_4,\eta_2,1)] \quad \text{(A29)}$$

$$\bar{g}_{\mathrm{AABB}}(x,\eta_2,\eta_3,\eta_4,h_2,h_3,h_4) = N^3\psi_4[f_{12}(x,\alpha,h_2,1,\eta_3) + f_{12}(x,\alpha,h_2,1,\eta_4) + f_{12}(x,\alpha,h_2,\eta_2,\eta_3) + f_{12}(x,\alpha,h_2,\eta_2,\eta_4)] + 2N^3\psi_2[f_{13}(x,\alpha,h_3,1,\eta_2) + f_{13}(x,\alpha,h_4,1,\eta_2)] \quad \text{(A30)}$$

$$\bar{g}_{\mathrm{BBAA}}(x,\eta_2,\eta_3,\eta_4,h_2,h_3,h_4) = N^3\psi_4[f_{12}(x,\alpha,h_2,\eta_3,1) + f_{12}(x,\alpha,h_2,\eta_4,1) + f_{12}(x,\alpha,h_2,\eta_3,\eta_2) + f_{12}(x,\alpha,h_2,\eta_4,\eta_2)] + 2N^3\psi_2[f_{13}(x,\alpha,h_3,\eta_3,\eta_4) + f_{13}(x,\alpha,h_4,\eta_3,\eta_4)] \quad \text{(A31)}$$

$$\bar{g}_{\mathrm{ABAB}}(x,\eta_2,\eta_3,\eta_4,h_2,h_3,h_4) = N^3\psi_4[f_{12}(x,\alpha,h_3,1,\eta_2) + f_{12}(x,\alpha,h_3,1,\eta_4) + f_{12}(x,\alpha,h_3,\eta_3,\eta_2) + f_{12}(x,\alpha,h_3,\eta_3,\eta_4)] + 2N^3\psi_2[f_{13}(x,\alpha,h_2,1,\eta_3) + f_{13}(x,\alpha,h_4,1,\eta_3)] \quad \text{(A32)}$$

$$\bar{g}_{\mathrm{BABA}}(x,\eta_2,\eta_3,\eta_4,h_2,h_3,h_4) = N^3\psi_4[f_{12}(x,\alpha,h_3,\eta_2,1) + f_{12}(x,\alpha,h_3,\eta_4,1) + f_{12}(x,\alpha,h_3,\eta_2,\eta_3) + f_{12}(x,\alpha,h_3,\eta_4,\eta_3)] + 2N^3\psi_2[f_{13}(x,\alpha,h_2,\eta_2,\eta_4) + f_{13}(x,\alpha,h_4,\eta_2,\eta_4)] \quad \text{(A33)}$$

$$\bar{g}_{\mathrm{ABBA}}(x,\eta_2,\eta_3,\eta_4,h_2,h_3,h_4) = N^3\psi_4[f_{12}(x,\alpha,h_4,1,\eta_2) + f_{12}(x,\alpha,h_4,1,\eta_3) + f_{12}(x,\alpha,h_4,\eta_4,\eta_2) + f_{12}(x,\alpha,h_4,\eta_4,\eta_3)] + 2N^3\psi_2[f_{13}(x,\alpha,h_2,1,\eta_4) + f_{13}(x,\alpha,h_3,1,\eta_4)] \quad \text{(A34)}$$

$$\bar{g}_{\mathrm{BAAB}}(x,\eta_2,\eta_3,\eta_4,h_2,h_3,h_4) = N^3\psi_4[f_{12}(x,\alpha,h_4,\eta_2,1) + f_{12}(x,\alpha,h_4,\eta_3,1) + f_{12}(x,\alpha,h_4,\eta_2,\eta_4) + f_{12}(x,\alpha,h_4,\eta_3,\eta_4)] + 2N^3\psi_2[f_{13}(x,\alpha,h_2,\eta_2,\eta_3) + f_{13}(x,\alpha,h_3,\eta_2,\eta_3)] \quad \text{(A35)}$$

where

$$f_6(x,\alpha,h,m,n) = \int_0^{\alpha} \mathrm{d}i \int_0^{i} \mathrm{d}j \int_0^{j} \mathrm{d}k \int_0^{k} \mathrm{d}l\ \mathrm{e}^{-mx(i-j)}\mathrm{e}^{-hx(j-k)}\mathrm{e}^{-nx(k-l)} \quad \text{(A36)}$$

$$f_7(x,\alpha,h,m,n) = \int_0^{1} \mathrm{d}i \int_{1+\alpha}^{2+\alpha} \mathrm{d}j \int_j^{2+\alpha} \mathrm{d}k \int_k^{2+\alpha} \mathrm{d}l\ \mathrm{e}^{-mx(j-i)}\mathrm{e}^{-hx(k-j)}\mathrm{e}^{-nx(l-k)} \quad \text{(A37)}$$

$$f_8(x,\alpha,h,m,n) = \int_0^{1} \mathrm{d}i \int_i^{1} \mathrm{d}j \int_{1+\alpha}^{2+\alpha} \mathrm{d}k \int_k^{2+\alpha} \mathrm{d}l\ \mathrm{e}^{-mx(j-i)}\mathrm{e}^{-hx(k-j)}\mathrm{e}^{-nx(l-k)} \quad \text{(A38)}$$

$$f_9(x,\alpha,h,m,n) = \int_0^{1} \mathrm{d}i \int_i^{1} \mathrm{d}j \int_j^{1} \mathrm{d}k \int_1^{1+\alpha} \mathrm{d}l\ \mathrm{e}^{-mx(j-i)}\mathrm{e}^{-hx(k-j)}\mathrm{e}^{-nx(l-k)} \quad \text{(A39)}$$

$$f_{10}(x,\alpha,h,m,n) = \int_0^{1} \mathrm{d}i \int_1^{1+\alpha} \mathrm{d}j \int_{1+\alpha}^{2+\alpha} \mathrm{d}k \int_k^{2+\alpha} \mathrm{d}l\ \mathrm{e}^{-mx(l-k)}\mathrm{e}^{-hx(k-j)}\mathrm{e}^{-nx(j-i)} \quad \text{(A40)}$$

$$f_{11}(x,\alpha,h,m,n) = \int_1^{1+\alpha} \mathrm{d}i \int_1^{i} \mathrm{d}j \int_1^{j} \mathrm{d}k \int_0^{1} \mathrm{d}l\ \mathrm{e}^{-mx(i-j)}\mathrm{e}^{-hx(j-k)}\mathrm{e}^{-nx(k-l)} \quad \text{(A41)}$$

$$f_{12}(x,\alpha,h,m,n) = \int_0^{1} \mathrm{d}i \int_i^{1} \mathrm{d}j \int_1^{1+\alpha} \mathrm{d}k \int_k^{1+\alpha} \mathrm{d}l\ \mathrm{e}^{-mx(j-i)}\mathrm{e}^{-hx(k-j)}\mathrm{e}^{-nx(l-k)} \quad \text{(A42)}$$

$$f_{13}(x,\alpha,h,m,n) = \int_0^{1} \mathrm{d}i \int_1^{1+\alpha} \mathrm{d}j \int_j^{1+\alpha} \mathrm{d}k \int_{1+\alpha}^{2+\alpha} \mathrm{d}l\ \mathrm{e}^{-mx(j-i)}\mathrm{e}^{-hx(k-j)}\mathrm{e}^{-nx(l-k)} \quad \text{(A43)}$$

Appendix B: Free Energy of Microstruture

In this Appendix, the formulas of $\Delta F_{\mathrm{micro}}$ for various structures are presented. The following notations will be used in the expressions for $\Delta F_{\mathrm{micro}}$:

$$\Gamma_3(\mathbf{q}_1,\mathbf{q}_2,\mathbf{q}_3) = \Gamma_3(x,\eta_2,\eta_3)$$
$$\Gamma_4(\mathbf{q}_1,\mathbf{q}_2,\mathbf{q}_3,\mathbf{q}_4) = \Gamma_4(x,\eta_2,\eta_3,\eta_4,h_2,h_3,h_4)$$
$$\boldsymbol{x}_1 = Q_1{}^2R^2 \quad \text{(B1)}$$

Furthermore, for convenience, the intrashell contributions of the vertexes, $\Gamma_3(x,1,1)$ and $\Gamma_4(x,1,1,1,h_2,h_3,h_4)$, are abbreviated as

$$\Gamma_3(x,1,1) = \Gamma_3(x)$$
$$\Gamma_4(x,1,1,1,h_2,h_3,h_4) = \Gamma_4(x,h_2,h_3,h_4) \quad \text{(B2)}$$

Following the notations above, the free energy densities of microstructure for various structures are given as follows.

For lamellar (L):

$$\frac{\Delta F_{\mathrm{micro}}}{Vk_{\mathrm{B}}T} = \Gamma_2(x_1)A_1{}^2 + \lambda_{1111}A_1{}^4 \quad \text{(B3)}$$

$$\lambda_{1111} = \frac{1}{4}\Gamma_4(x_1,0,0,4) \quad \text{(B4)}$$

For hexagonal (H):

$$\frac{\Delta F_{\mathrm{micro}}}{Vk_{\mathrm{B}}T} = \Gamma_2(x_1)A_1{}^2 + \nu_{111}A_1{}^3 + \lambda_{1111}A_1{}^4 \quad \text{(B5)}$$

$$\nu_{111} = -\frac{2}{3\sqrt{3}}|\Gamma_3(x_1)| \quad \text{(B6)}$$

$$\lambda_{1111} = \frac{1}{12}\Gamma_4(x_1,0,0,4) + \frac{1}{3}\Gamma_4(x_1,0,1,3) \quad \text{(B7)}$$

For square (SQ):

$$\frac{\Delta F_{\text{micro}}}{Vk_{\text{B}}T} = \Gamma_2(x_1){A_1}^2 + \Gamma_2(2x_1){A_2}^2 + 3\nu_{112}{A_1}^2A_2 + \lambda_{1111}{A_1}^4 + 6\lambda_{1122}{A_1}^2{A_2}^2 + \lambda_{2222}{A_2}^4 \quad \text{(B8)}$$

$$\nu_{112} = -\frac{2}{3\sqrt{2}}|\Gamma_3(x_1,1,2)| \quad \text{(B9)}$$

$$\lambda_{1111} = \frac{1}{8}\Gamma_4(x_1,0,0,4) + \frac{1}{4}\Gamma_4(x_1,0,2,2) \quad \text{(B10)}$$

$$\lambda_{1122} = \frac{1}{6}\Gamma_4(x_1,1,2,2,0,1,5) + \frac{1}{12}\Gamma_4(x_1,1,2,2,4,1,1) \quad \text{(B11)}$$

$$\lambda_{2222} = \frac{1}{8}\Gamma_4(2x_1,0,0,4) + \frac{1}{4}\Gamma_4(2x_1,0,2,2) \quad \text{(B12)}$$

For body-centered cubic (B):

$$\frac{\Delta F_{\text{micro}}}{Vk_{\text{B}}T} = \Gamma_2(x_1){A_1}^2 + \Gamma_2(2x_1){A_2}^2 + \nu_{111}{A_1}^3 + 3\nu_{112}{A_1}^2A_2 + \lambda_{1111}{A_1}^4 + 4\lambda_{1112}{A_1}^3A_2 + 6\lambda_{1122}{A_1}^2{A_2}^2 + \lambda_{2222}{A_2}^4 \quad \text{(B13)}$$

$$\nu_{111} = -\frac{4}{3\sqrt{6}}|\Gamma_3(x_1)| \quad \text{(B14)}$$

$$\nu_{112} = -\frac{2}{3\sqrt{3}}|\Gamma_3(x_1,1,2)| \quad \text{(B15)}$$

$$\lambda_{1111} = \frac{1}{24}\Gamma_4(x_1,0,0,4) + \frac{1}{3}\Gamma_4(x_1,0,1,3) + \frac{1}{12}\Gamma_4(x_1,0,2,2) + \frac{1}{6}\Gamma_4(x_1,1,2,1) \quad \text{(B16)}$$

$$\lambda_{1112} = \frac{1}{3\sqrt{2}}\Gamma_4(x_1,1,1,2,1,1,3) \quad \text{(B17)}$$

$$\lambda_{1122} = \frac{1}{9}\Gamma_4(x_1,1,2,2,0,1,5) + \frac{1}{18}\Gamma_4(x_1,1,2,2,0,3,3) + \frac{1}{18}\Gamma_4(x_1,1,2,2,4,1,1) \quad \text{(B18)}$$

$$\lambda_{2222} = \frac{1}{12}\Gamma_4(2x_1,0,0,4) + \frac{1}{3}\Gamma_4(2x_1,0,2,2) \quad \text{(B19)}$$

For face-centered cubic (*F*):

$$\frac{\Delta F_{\text{micro}}}{Vk_{\text{B}}T} = \Gamma_2(x_1){A_1}^2 + \Gamma_2({}^4/_3x_1){A_2}^2 + 3\nu_{112}{A_1}^2A_2 + \lambda_{1111}{A_1}^4 + 6\lambda_{1122}{A_1}^2{A_2}^2 + \lambda_{2222}{A_2}^4 \quad \text{(B20)}$$

$$\nu_{112} = -\frac{1}{\sqrt{3}}|\Gamma_3(x_1,1,{}^4/_3)| \quad \text{(B21)}$$

$$\lambda_{1111} = \frac{1}{16}\Gamma_4(x_1,0,0,4) + \frac{3}{8}\Gamma_4(x_1,0,{}^4/_3,{}^8/_3) + \frac{1}{8}\Gamma_4(x_1,{}^4/_3,{}^4/_3,{}^4/_3) \quad \text{(B22)}$$

$$\lambda_{1122} = \frac{1}{6}\Gamma_4(x_1,1,{}^4/_3,{}^4/_3,0,1,{}^{11}/_3) + \frac{1}{6}\Gamma_4(x_1,1,{}^4/_3,{}^4/_3,{}^8/_3,1,1) \quad \text{(B23)}$$

For simple cubic (SC):

$$\frac{\Delta F_{\text{micro}}}{Vk_{\text{B}}T} = \Gamma_2(x_1){A_1}^2 + \Gamma_2(2x_1){A_2}^2 + 3\nu_{112}{A_1}^2A_2 + \nu_{222}{A_2}^3 + \lambda_{1111}{A_1}^4 + 6\lambda_{1122}{A_1}^2{A_2}^2 + \lambda_{2222}{A_2}^4 \quad \text{(B24)}$$

$$\nu_{222} = -\frac{4}{3\sqrt{6}}|\Gamma_3(2x_1)| \quad \text{(B25)}$$

$$\nu_{112} = -\frac{4}{3\sqrt{6}}|\Gamma_3(x_1,1,2)| \quad \text{(B26)}$$

$$\lambda_{1111} = \frac{1}{12}\Gamma_4(x_1,0,0,4) + \frac{1}{3}\Gamma_4(x_1,0,2,2) \quad \text{(B27)}$$

$$\lambda_{1122} = \frac{1}{9}\Gamma_4(x_1,1,2,2,0,1,5) + \frac{1}{18}\Gamma_4(x_1,1,2,2,0,3,3) + \frac{2}{9}\Gamma_4(x_1,1,2,2,2,1,3) + \frac{1}{18}\Gamma_4(x_1,1,2,2,4,1,1) \quad \text{(B28)}$$

$$\lambda_{2222} = \frac{1}{24}\Gamma_4(2x_1,0,0,4) + \frac{1}{3}\Gamma_4(2x_1,0,1,3) + \frac{1}{12}\Gamma_4(2x_1,0,2,2) + \frac{1}{6}\Gamma_4(2x_1,1,2,1) \quad \text{(B29)}$$

For hexagonally perforated lamellar (HPL):

$$\frac{\Delta F_{\text{micro}}}{Vk_{\text{B}}T} = \Gamma_2(x_1){A_1}^2 + \Gamma_2(dx_1){A_2}^2 + \nu_{111}{A_1}^3 + \lambda_{1111}{A_1}^4 + 6\lambda_{1122}{A_1}^2{A_2}^2 + \lambda_{2222}{A_2}^4 \quad \text{(B30)}$$

$$\nu_{111} = -\frac{2}{3\sqrt{3}}|\Gamma_3(x_1)| \quad \text{(B31)}$$

$$\lambda_{1111} = \frac{1}{12}\Gamma_4(x_1,0,0,4) + \frac{1}{3}\Gamma_4(x_1,0,1,3) \quad \text{(B32)}$$

$$\lambda_{1122} = \frac{1}{6}\Gamma_4(x_1,1,d,d,0,1+d,1+d) \quad \text{(B33)}$$

$$\lambda_{2222} = \frac{1}{4}\Gamma_4(dx_1,0,0,4) \quad \text{(B34)}$$

For double gyroid (G):

$$\frac{\Delta F_{\text{micro}}}{Vk_{\text{B}}T} = \Gamma_2(x_1){A_1}^2 + \Gamma_2({}^4/_3x_1){A_2}^2 + \nu_{111}{A_1}^3 + 3\nu_{112}{A_1}^2A_2 + \nu_{222}{A_2}^3 + \lambda_{1111}{A_1}^4 + 4\lambda_{1112}{A_1}^3A_2 + 6\lambda_{1122}{A_1}^2{A_2}^2 + \lambda_{2222}{A_2}^4 \quad \text{(B35)}$$

$$\nu_{111} = -\frac{1}{3\sqrt{3}}|\Gamma_3(x_1)| \quad \text{(B36)}$$

$$\nu_{112} = \frac{1}{3\sqrt{6}}|\Gamma_3(x_1,1,{}^4/_3)| \quad \text{(B37)}$$

$$\nu_{222} = -\frac{4}{3\sqrt{6}}|\Gamma_3(({}^4/_3)x_1)| \quad \text{(B38)}$$

$$\lambda_{1111} = \frac{1}{48}\Gamma_4(x_1,0,0,4) + \frac{1}{12}\Gamma_4(x_1,0,{}^1/_3,{}^{11}/_3) + \frac{1}{12}\Gamma_4 \times (x_1,0,{}^2/_3,{}^{10}/_3) + \frac{1}{12}\Gamma_4(x_1,0,1,3) + \frac{1}{24}\Gamma_4(x_1,0,{}^4/_3,{}^8/_3) + \frac{1}{6}\Gamma_4(x_1,0,{}^5/_3,{}^7/_3) - \frac{1}{12}\Gamma_4(x_1,{}^1/_3,{}^2/_3,3) - \frac{1}{12}\Gamma_4 \times (x_1,{}^2/_3,{}^5/_3,{}^5/_3) + \frac{1}{24}\Gamma_4(x_1,{}^2/_3,{}^8/_3,{}^2/_3) \quad \text{(B39)}$$

$$\lambda_{1112} = -\frac{1}{12\sqrt{2}}\Gamma_4(x_1,1,1,{}^4/_3,{}^1/_3,{}^1/_3,{}^{11}/_3) + \frac{1}{6\sqrt{2}}\Gamma_4 \times (x_1,1,1,{}^4/_3,{}^1/_3,{}^5/_3,{}^7/_3) - \frac{1}{12\sqrt{2}}\Gamma_4(x_1,1,1,{}^4/_3,1,{}^5/_3,{}^5/_3) \quad \text{(B40)}$$

$$\lambda_{1122} = \frac{1}{18}\Gamma_4(x_1,1,{}^4/_3,{}^4/_3,0,{}^1/_3,{}^{13}/_3) + \frac{1}{36}\Gamma_4(x_1,1,{}^4/_3,{}^4/_3,0,1,{}^{11}/_3) + \frac{1}{18}\Gamma_4(x_1,1,{}^4/_3,{}^4/_3,0,{}^5/_3,3) + \frac{1}{36}\Gamma_4(x_1,1,{}^4/_3,{}^4/_3,0,{}^7/_3,{}^7/_3) - \frac{1}{18}\Gamma_4(x_1,1,{}^4/_3,{}^4/_3,{}^4/_3,{}^1/_3,3) - \frac{1}{18}\Gamma_4(x_1,1,{}^4/_3,{}^4/_3,{}^8/_3,{}^1/_3,3) + \frac{1}{36}\Gamma_4(x_1,1,{}^4/_3,{}^4/_3,4,{}^1/_3,{}^1/_3) \quad \text{(B41)}$$

$$\lambda_{2222} = \frac{1}{24}\Gamma_4({}^4/_3x_1,0,0,4) + \frac{1}{3}\Gamma_4({}^4/_3x_1,0,1,3) + \frac{1}{12}\Gamma_4({}^4/_3x_1,0,2,2) + \frac{1}{6}\Gamma_4({}^4/_3x_1,1,2,1) \quad \text{(B42)}$$

For double diamond (OBDD):

$$\frac{\Delta F_{\text{micro}}}{Vk_BT} = \Gamma_2(x_1)A_1{}^2 + \Gamma_2({}^3/_2x_1)A_2{}^2 + \nu_{111}A_1{}^3 + \lambda_{1111}A_1{}^4 + 6\lambda_{1122}A_1{}^2A_2{}^2 + \lambda_{2222}A_2{}^4 \quad \text{(B43)}$$

$$\nu_{111} = -\frac{4}{3\sqrt{6}}|\Gamma_3(x_1)| \quad \text{(B44)}$$

$$\lambda_{1111} = \frac{1}{24}\Gamma_4(x_1,0,0,4) + \frac{1}{3}\Gamma_4(x_1,0,1,3) + \frac{1}{12}\Gamma_4(x_1,0,2,2) + \frac{1}{6}\Gamma_4(x_1,1,2,1) \quad \text{(B45)}$$

$$\lambda_{1122} = \frac{1}{12}\Gamma_4(x_1,1,{}^3/_2,{}^3/_2,0,{}^1/_2,{}^9/_2) + \frac{1}{12}\Gamma_4(x_1,1,{}^3/_2,{}^3/_2,0,{}^5/_2,{}^5/_2) - \frac{1}{6}\Gamma_4(x_1,1,{}^3/_2,{}^3/_2,2,{}^1/_2,{}^5/_2) + \frac{1}{24}\Gamma_4(x_1,1,{}^3/_2,{}^3/_2,4,{}^1/_2,{}^1/_2) \quad \text{(B46)}$$

$$\lambda_{2222} = \frac{1}{16}\Gamma_4({}^3/_2x_1,0,0,4) + \frac{3}{8}\Gamma_4({}^3/_2x_1,0,{}^4/_3,{}^8/_3) + \frac{1}{8}\Gamma_4({}^3/_2x_1,{}^4/_3,{}^4/_3,{}^4/_3) \quad \text{(B47)}$$

References and Notes

(1) Helfand, E.; Wasserman, Z. R. *Developments in Block Copolymers*; Goodman, I., Ed.; Applied Science: New York, 1987.
(2) Bates, F. S.; Fredrickson, G. H. *Annu. Rev. Phys. Chem.* **1990**, *41*, 525.
(3) Hamley, I. W. *The Physics of Block Copolymers*; Oxford University Press: Oxford, England, 1998.
(4) Ikkala, O.; ten Brinke, G. *Science* **2002**, *295*, 2407.
(5) Ruokolainen, J.; Mäkinen, R.; Torkkeli, M.; Mäkelä, T.; Serimaa, R.; ten Brinke, G.; Ikkala, O. *Science* **1998**, *280*, 557.
(6) Russell, T. P.; Jerome, R.; Charlier, P.; Foucart, M. *Macromolecules* **1988**, *21*, 1709.
(7) Iwasaki, K.; Hirao, A.; Nakahama, S. *Macromolecules* **1993**, *26*, 2126.
(8) Alexander, C.; Jariwala, C. P.; Lee, C. M.; Griffith, A. C. *Macromol. Symp.* **1994**, *77*, 283.
(9) Ruokolainen, J.; ten Brinke, G.; Ikkala, O.; Torkkeli, M.; Serimaa, R. *Macromolecules* **1996**, *29*, 3409.
(10) Pipas, S.; Floudas, G.; Pakula, T.; Lieser, G.; Sakellariou, S.; Hadjichristidis, N. *Macromolecules* **2003**, *36*, 759.
(11) Tanaka, F.; Ishida, M.; Matsuyama, A. *Macromolecules* **1991**, *24*, 5582.
(12) Tanaka, F.; Ishida, M. *Macromolecules* **1997**, *30*, 1836.
(13) Shoji, M.; Tanaka, F. *Macromolecules* **2002**, *35*, 7460.
(14) Dormidontova, E.; ten Brinke, G. *Macromolecules* **1998**, *31*, 2649.
(15) Angerman, H. J.; ten Brinke, G. *Macromolecules* **1999**, *32*, 6813.
(16) Leibler, L. *Macromolecules* **1980**, *13*, 1602.
(17) Panyukov, S. V.; Kuchanov, S. I. *JETP Lett.* **1991**, *54*, 501.
(18) Panyukov, S. V.; Kuchanov, S. I. *JETP* **1991**, *72*, 368.
(19) Erukhimovich, I. Ya.; Dobrynin, A. V. *Macromol. Symp.* **1991**, *81*, 253.
(20) Milner, S. T.; Olmsted, P. D. *J. Phys. II Fr.* **1991**, *81*, 253.
(21) Olvera de la cruz, M.; Mayes, A. M.; Swift, B. W. *Macromolecules* **1992**, *25*, 944.
(22) Hamley, I. W.; Bates, F. S. *J. Chem. Phys.* **1994**, *100*, 6813.
(23) Aksimentiev, A.; Holyst, R. *J. Chem. Phys.* **1999**, *111*, 2329.
(24) Pimentel, G. C.; McClellan, A. L. *Annu. Rev. Phys. Chem.* **1971**, *22*, 347.
(25) Coleman, M. M.; Graf, J. F.; Painter, P. C. *Specific Interactions and the Miscibility of Polymer Blends*; Technomic Pub. Co.: Lancaster, PA, 1991.
(26) Moriyoski, T.; Kaneshina, S.; Aihara, K.; Yabumoto, K. *J. Chem. Thermodyn.* **1975**, *7*, 537.
(27) Dolgolenko, W. *J. Phys. Chem.* **1980**, *62*, 339.
(28) Marques, C. M.; Cates, M. E. *Europhys. Lett.* **1990**, *13*, 267.
(29) Matsen, M. W. *Macromolecules* **1995**, *28*, 5765.

MA034895M